Behavior of Retrofitted URM Walls under Simulated Earthquake Loading

By M. R. Ehsani,[1] Fellow, ASCE, H. Saadatmanesh,[2] Member, ASCE, and J. I. Velazquez-Dimas[3]

ABSTRACT: Unreinforced masonry (URM) buildings perform poorly under seismic forces and have been identified as the main cause of loss of life in recent earthquakes. Many of these structures fail in out-of-plane bending due to the lack of reinforcement. In this study, the experimental results from three half-scale unreinforced brick walls retrofitted with vertical composite strips are presented. The specimens were subjected to cyclic out-of-plane loading. Five reinforcement ratios and two different glass fabric composite densities were investigated. The mode of failure is controlled by tensile failure when wider and lighter composite fabrics are used and by delamination when stronger ones are used. The tested specimens were capable of supporting a lateral load up to 32 times the weight of the wall. A deflection as much as 2% of the wall height was measured. Although both URM walls and composite strips behave in a brittle manner, the combination resulted in a system capable of dissipating some energy. Retrofitting URM walls with composite strips proved to be a good and reliable strengthening alternative.

INTRODUCTION

General

Being one of the oldest and most widely used types of construction materials in the world, masonry deserves to be rediscovered by modern engineering technology. Inherent advantages, e.g., aesthetics, architectural appearance, effective heat and sound insulation, fire resistance, and economical construction, will contribute to the use of masonry as the prime construction material, especially for residential construction once its mechanical behavior is well understood (Sucuoglu and McNiven 1991). There is a large inventory of unreinforced masonry (URM) buildings in the world. Most of these were built with little or no seismic loading requirement, and they are not capable of dissipating energy through inelastic deformation during earthquakes.

As shown in Fig. 1, in most older buildings, the floor joists simply rest on the masonry wall. During the earthquake, the wall movement would result in loss of support for the beam. One method to fix this problem is to bolt some of the floor joists through the wall. This retrofitting technique has been applied to many buildings in California since the mid 1980s. The retrofitted buildings can be easily identified from the washers that are used on the exterior face of the wall. The intent is to force the wall to span between floors. However, because most of these walls do not contain any reinforcement, they cannot resist the imposed loads and displacements. The result is that many of these retrofitted buildings are subject to severe damage in future earthquakes (Fig. 2); in essence, the weakest link in the chain that used to be the connection between the wall and the floor has been replaced with the unreinforced wall itself. These continuing challenges have resulted in URM buildings being identified as the primary cause of injuries and loss of life (Tobriner 1984; Deppe 1988; *Expected* 1994; Kehoe 1996; Tomazevic 1996).

Two types of failure are commonly observed in load bearing

URM walls subjected to seismic loads. These are in-plane failure characterized by a diagonal tensile crack pattern, and the out-of-plane failure, where cracks are primarily along the mortar bed joints; some inclined cracks may also be developed. The exact crack pattern will, of course, depend on the wall boundary conditions. Between these two, the out-of-plane failure has been identified as the main cause of loss of lives. Therefore, there is a necessity for better understanding of this failure as well as for development of new and more efficient retrofitting techniques. In the present paper, the experimental results of three half-scale URM walls retrofitted with E-glass fiber-reinforced polymer (GFRP) strips and tested under cyclic out-of-plane bending are presented.

LITERATURE REVIEW

The potential out-of-plane failure of URM elements such as parapet walls, veneers, and unanchored load bearing walls during earthquakes constitutes the most serious life-safety hazard for this type of construction. Whereas an in-plane failure does not usually endanger the gravity load carrying capacity of the wall, the unstable and explosive out-of-plane failure will (Bruneau 1994). Consequently, URM buildings are more vulnerable to out-of-plane failure. Many researchers have concluded that there are still insufficient experimental and theoretical results for masonry walls uniformly loaded in the lateral direction (Hendry 1973; Bennedetti and Benzoni 1984; Essaway 1986; Dawe and Seah 1989; Hamid et al. 1992; Flanagan et al. 1993; Abrams et al. 1993; Drysdale et al. 1994).

One of the most important experimental and analytical studies on out-of-plane bending of URM walls is that developed by ABK ("Methodology" 1981). In this study, dynamic analysis as well as dynamic tests were performed on URM walls. The main objective was to develop a methodology for mitigation of seismic hazard in URM buildings. Twenty wall spec-
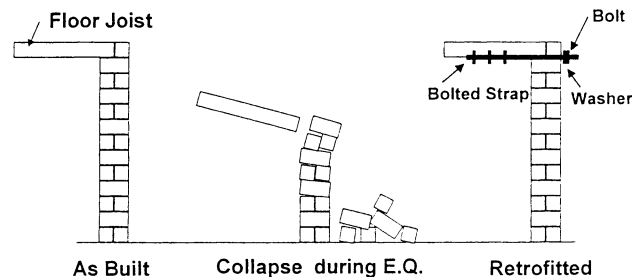
FIG. 1. Failure and Retrofit of URM Walls

FIG. 2. Failure of URM Wall That Was Retrofitted by Tying Floor Beams to Wall

imens from the most representative URM buildings were subjected to dynamic out-of-plane motions. From the observed behavior, upper-bound values were established for the dynamic stability of masonry panels. Typical values for the height-to-thickness ratios found in different seismic zones were established. These were incorporated into some codes such as the Uniform Code for Building Conservation (*Uniform* 1994) and the NEHRP *Handbook for seismic rehabilitation of existing buildings* (1992; Bruneau 1994).

Although GFRP offers great potential in increasing strength and ductility of masonry walls, few studies have been conducted on URM walls retrofitted with glass-fabric overlays. Earlier studies have demonstrated that the static bending capacity of URM beams can be significantly increased by epoxy bonding a sheet of GFRP to the tension face (Ehsani and Saadatmanesh 1994). The study presented here was conducted to demonstrate the feasibility of such a retrofitting system for structures subjected to reverse cyclic loading.

STRENGTHENING TECHNIQUES FOR URM WALLS

Conventional Methods

Several retrofitting approaches are available to increase the strength and ductility of masonry buildings. A comprehensive survey of all of these techniques was recently completed (Lizundia et al. 1997). These can be categorized in two types (*Handbook* 1992). The first relates to adding structural elements such as steel or concrete frames to the existing building. This option presents some disadvantages such as adding significant weight to the building, which in turn may require foundation adjustments, resulting in higher retrofit costs. Another disadvantage is that valuable space is lost to the framing elements, and in some cases, disturbance of the occupants may occur. Siegel and Fowler (1994) reported that an eccentric concrete frame was used for repairing a five-story URM building damaged during the Loma Prieta earthquake.

The second alternative is related to surface treatments. This alternative can be achieved in many ways. A standard procedure consists of removing one wythe form the existing multiwythe wall and replacing it by a layer of reinforced concrete (or gunite). In some cases, the walls are retrofitted with steel plates attached to the wall with steel anchors.

Among major studies using surface coating is one by Abrams et al. (1994) that used a ferrocement plaster coating on slender masonry walls in combination with a single sheet of hardware steel mesh. They found that this technique enhanced the ultimate flexural capacity of the panels as much as 2.5 times with respect to the control specimen. Bhende and Ovadia (1994) used steel plates attached to eight URM walls

with steel anchors in a nuclear power plant facility. Test results indicated that the out-of-plane capacity of the walls was increased by a factor of 10 compared to the nonretrofitted ones. However, they suggested that the effect of drilled holes on in-plane behavior needs to be addressed.

Strengthening with FRPs

There is a variation of surface treatments where fiber-reinforced polymer (FRP) materials are used in the form of overlays or plates on masonry walls; similar to many other construction techniques, this invention has been patented (U.S. Patent No. 5,640,825; Lester 1998). FRPs are made of strong fibers such as glass, carbon, and aramid bound by an epoxy resin or polyester. The main function of the fibers is to carry the applied load; the matrix protects the fibers from damage and distributes the load among fibers. Composite materials are very attractive for construction applications due to their superior characteristics with respect to conventional materials such as steel. Among them are a high strength-to-weight ratio, corrosion resistance, and ease of application. They also have some disadvantages, such as low shear strength, potential for ultraviolet degradation, and deterioration at high temperatures.

There are a few reported studies and field applications of composites on masonry buildings. However, most of the studies reported are for in-plane masonry walls retrofitted with either carbon or glass overlays (Weeks et al. 1994; Laursen et al. 1995; Schwegler 1995; Ehsani and Saadatmanesh 1997). In all cases, composites have demonstrated good performance in increasing the shear behavior of masonry elements. Only one study has been reported where glass-fabric was used on brick masonry walls under transverse load (Ehsani and Saadatmanesh 1994). In this study, several brick masonry beams retrofitted with glass-fabric sheets were tested. This technique improved the ultimate flexural strength so that the beam could resist a load 20 times its weight; deflections were as much as 1/50 of the span.

In addition, three field applications have been reported (Ehsani and Saadatmanesh 1996; Schwegler and Kelterborn 1996; Ehsani and Saadatmanesh 1997). In the first application, glass-fabric overlays were bonded on both faces of the walls of a concrete block masonry building that was damaged during the Northridge earthquake. In the second application, a 60-year-old and six-story residential brick masonry building was retrofitted with carbon fiber-reinforced plastic (CFRP) sheets in order to overcome the new seismic demand. This was done because the building was remodeled as an office building. Ehsani and Saadatmanesh (1997) reported the latest and largest field application of composite fabrics on tilt-up concrete masonry walls of a building damaged during the Northridge earthquake. Nearly 20,000 sq ft of wall surface were retrofitted with glass composite fabric in this building. In all cases, retrofitting with composite material has proven to be an efficient and cost-competitive technique.
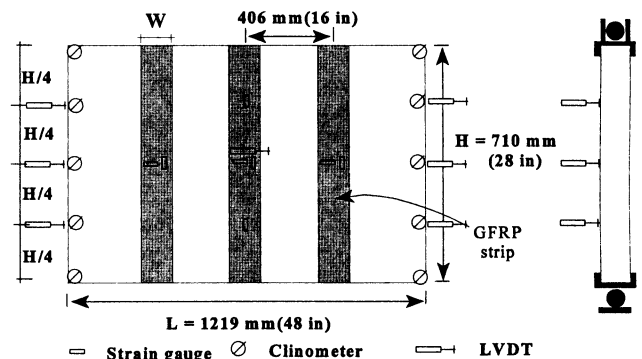

FIG. 3. Overall View of Test Specimens and Instrumentation

TABLE 1. Overall Wall Parameters

Specimen designation (1)	Length [mm (in.)] (2)	Height [mm (in.)] (3)	h/t (4)	% ρ_b South face (5)	% ρ_b North face (6)	Fabric Width (W) [mm (in.)] South face (7)	Fabric Width (W) [mm (in.)] North face (8)	w/t South face (9)	w/t North face (10)
S75/25	1,220 (48)	710 (28)	14	25	75	34 (1.33)	101 (3.98)	0.7	2.1
S40/20	1,220 (48)	710 (28)	14	40	20	54 (2.12)	27 (1.06)	1.11	0.55
S30/30	1,220 (48)	710 (28)	41	30	30	81 (3.18)	81 (3.18)	1.7	1.7

Note: h = height, t = thickness, and ρ_b = balanced reinforcement ratio.

TABLE 2. Material Properties

Component (1)	Measured property (2)	Measured value (3)	Coefficient of variation (%) (4)
Brickwork	Density [kN/m³ (lb/cu ft)]	18.7 (120)	0.85
Mortar, ASTM C270-92	Compression capacity [kPa (psi)]	5,190 (754)[a]	12.5
Mortar, ASTM C270-92	Compression capacity [kPa (psi)]	7,200 (1,044)[b]	23
Brick units, ASTM C-67	Compression capacity [MPa (ksi)]	45 (5.51)	12.2
Brick units, ASTM C-67	Initial rate of absorption (g/min)	7.9	20.2
Brick prisms, ASTM E447-80	Compression capacity [MPa (ksi)]	20 (2.9)[a]	9.6
Brick prisms, ASTM E447-80	Compression capacity [MPa (ksi)]	26.7 (3.87)[b]	11.2
Brick beams, ASTM E518-80	Modulus of rupture [kPa (psi)]	1,482 (215)[a]	24.4
Brick beams, ASTM E518-80	Modulus of rupture [kPa (psi)]	1,613 (234)[b]	11

[a]Measured at 28 days.
[b]Measured at testing time.

EXPERIMENTAL INVESTIGATION

Test Specimens

Three half-scale unreinforced masonry walls were constructed with solid clay brick. As shown in Fig. 3, the specimens were 0.710 m (28 in.) high and 1.22 m (48 in.) long. They were constructed in a single wythe of 49 × 38 × 102 mm (1.92 × 1.5 × 4 in.) reduced-scale solid clay bricks with cement-lime type N mortar. As illustrated in Table 1, each wall is designated with the letter "S" followed by two numbers. The letter S refers to single wythe; the following two numbers refer to the percentage of composite reinforcement with respect to the balanced condition used on the south and the north faces of the wall, respectively. A balanced condition is assumed to occur when the compressive capacity of brickwork is reached at the same time that the composite material reaches its tensile capacity. All specimens were retrofitted with vertical E-glass fabric composite strips bonded on both faces of the walls with a two-component epoxy resin.

Wall Construction and Retrofitting

To reproduce field conditions as closely as possible, a mason and his assistant were hired for constructing the specimens. Solid clay masonry bricks were used, similar to those found in the majority of old URM buildings. These were bonded with a low-strength type N mortar. Reduced-scale bricks were carefully cut to exact dimensions from pavement bricks supplied by a local brick manufacturer.

Scaled models have been successfully used in many research projects (Abboud et al. 1990; Abrams et al. 1993; Abrams and Costley 1996) to study the behavior of full-scale prototypes. The bricks were laid in running bond with a mortar joint of 0.25 in. thickness to match the reduced-scale brick dimensions. River sand was used for the mortar mixture. The first course of bricks for all specimens was placed in a machined steel channel that formed a part of the support during the test. As can be seen in Fig. 3, all walls were simply supported at the top and bottom, and the other two sides remained free. The test specimens were intended to represent a portion of a typical load-bearing wall in a low-rise building away from corners.

All specimens were retrofitted with vertical composite strips of E-glass. These were bonded to the wall surface with an epoxy resin using the wet lay-up procedure. The steps followed were as follows: First, the wall was cleaned with a steel brush, and dust and any loose particles were removed with high air pressure. The surface of the wall where the fabrics

TABLE 3. Tensile Capacity of Fabrics

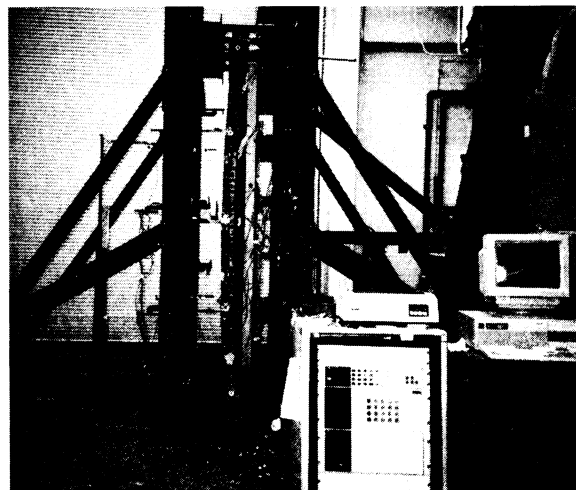| Fabric description (1)	18 oz Unidirectional Measured value (2)	18 oz Unidirectional COV (%) (3)	18 oz Cross-Ply (0/90) Measured value (4)	18 oz Cross-Ply (0/90) COV (%) (5)
P_u [N/mm (lb/in.)]	370 (2,106)	4.3	184 (1,053)	3.6
σ_u [MPa (ksi)]	197 (28.6)	5.0	93 (13.6)	5.4
ε_u (%)	1.85	10	1.6	11.6
E [GPa (ksi)]	10.3 (1,500)	5.0	5.9 (855)	11.0

Note: COV = coefficient of variation.

FIG. 4. Test Frame

were to be attached was coated with a thin layer of a two-component water-based primer. Second, composite fabric strips were cut and laid on a plastic sheet, and the mixed epoxy was poured on the fabric and spread over the whole fabric using a trowel, ensuring that the fabric was saturated with epoxy. Next, the saturated composite strips were bonded to the wall surface by hand pressure and pressed with a roller. Finally, a small layer of epoxy was put on the fabric for protection and instrumentation purposes. This retrofitting process was followed for the three walls. As depicted in Fig. 3, the

center-to-center space between vertical strips was kept constant at 406 mm (16 in.) for all specimens. The fabric width varied for different reinforcement ratios. These values can be observed in Table 1.

Material Properties

The material properties were characterized according to the appropriate ASTM standards. For the brick units, compressive strength and initial rate of absorption (IRA) were determined, and are shown in Table 2. Due to relatively high IRA values, the bricks were soaked in water prior to construction. This reduced the IRA and ensured a better bond between the mortar and the bricks. For the brick-mortar assemblages, the compressive strength was determined using prisms constructed with five bricks, and the modulus of rupture was obtained using beam specimens constructed with 10 bricks. The properties were obtained at 28 days and at testing time, as shown in Table 2.

From the specimens for modulus of rupture, the density for brickwork was also determined. The compression capacity for mortar was determined at 28 days and at testing time; more details about material properties can be found elsewhere (Velazquez-Dimas 1998). To achieve the 0.25 in. mortar bed, a sieve analysis was carried out for the sand used in the mortar. Sand passing mesh number 18 was used in the mortar. The tensile strength for both composite fabrics used in the present study was determined, and the corresponding values are shown
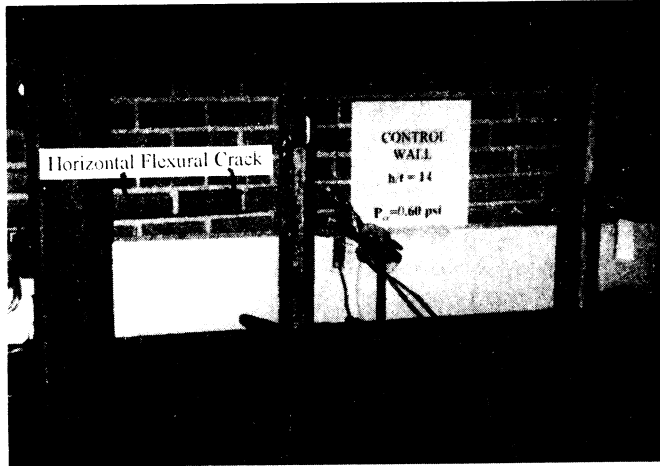

FIG. 5.   Failure of Control Specimen

(a)   Deflection (in.)

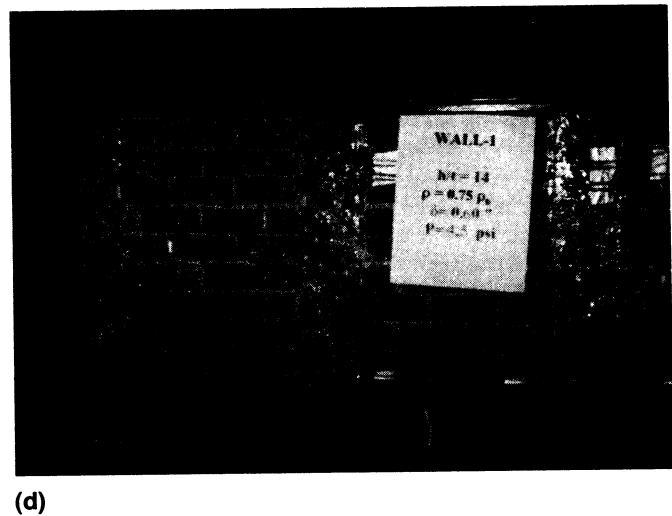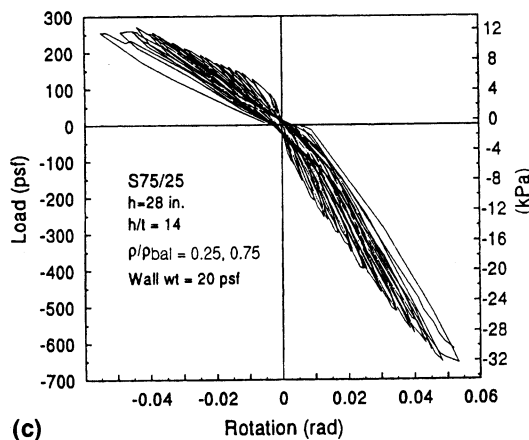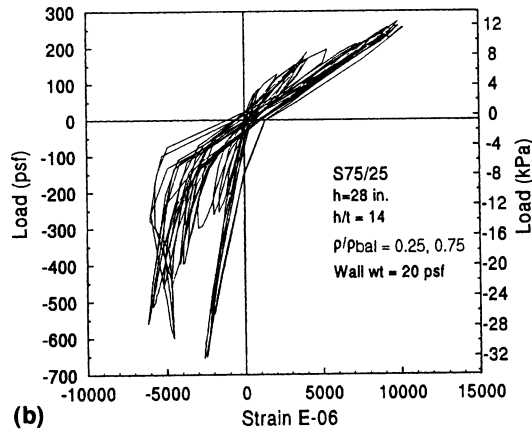(b)   Strain E-06
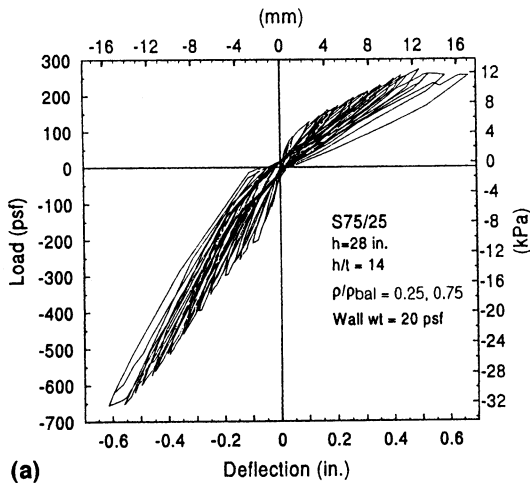

(c)   Rotation (rad)

(d)

FIG. 6.   Specimen S75/25: (a) Load versus Deflection at Midheight; (b) Load versus Longitudinal Strain in GFRP Strip; (c) Load versus Rotation at Top Support; (d) Delamination and Crack Patterns Just before Failure

in Table 3. As expected, the stress-strain relationship for the composite fabrics was linear to failure.

Test Setup and Instrumentation

A steel test frame capable of accommodating specimens up to 3,060 mm (120 in.) high was constructed. The testing frame consisted of two identical reaction frames, one in the north and one in the south. These reaction frames were spaced 920 mm (36 in.) apart to provide space for the placement of the wall specimen and the airbag. Each reaction frame consisted of three W8 × 31 columns, nine W8 × 31 cross beams, and three bracing elements built with C3 × 8 channels. An airbag confined in a plywood box was used for applying the out-of-plane pressure to the wall surfaces. The test frame is shown in Fig. 4. However, the wall shown in the photograph is a taller wall that is not discussed in the present paper.

The three walls were instrumented identically. As shown in Fig. 3, 10 strain gauges (SG1–SG10) were used to monitor longitudinal and transverse strains on the north and the south faces of the wall at five points in the composite strips. Ten clinometers (C1–C10) were also attached along the height of the wall on the east and west wall edges to measure rotations. Seven points were instrumented with linear variable displacement transducer (LVDTs) to measure out-of-place displacements. In addition, a pressure sensor capable of measurements with an accuracy of 0.35 kPa (0.05 psi) was connected to the airbag for measuring the applied pressure. Data from all devices were recorded through a computer-controlled data-acquisition system.

Loading History

Each wall was subjected to a prescribed out-of-plane load and displacement history. No axial load was applied to the walls to exclude the beneficial effect of axial compressive stresses on the mortar. The load sequence consisted of a large number of cyclic displacements. The first four cycles were applied under the load-controlled mode, two before cracking and two for the cracking load. The remaining cycles were applied under a displacement-controlled mode. The specimens were subjected to a maximum displacement of 1.3 mm (0.05 in.) during the first cycle. This increment was selected considering the estimated failure deflection of the wall, and to ensure that the specimens could be subjected to approximately 20 displacement cycles. The walls were subjected to two cycles at each maximum displacement level to evaluate the stiffness degradation of the wall. The maximum displacement for the next pair of cycles was increased by 1.3 mm (0.05 in.). This procedure was followed until failure of the wall was reached.

The lateral load was applied to the wall by means of an airbag system. Each cycle began by gradually pressurizing the airbag on the north face of the wall (i.e., the south face of the wall subjected to tension). After reaching the maximum load or displacement, the airbag was gradually depressurized to zero pressure. For the second half of the cycle, the airbag and the confining box were moved to the south face of the wall, and the procedure was repeated. These movements were necessary in order to have access to the tension face of the wall to monitor and record cracks and delamination patterns.

EXPERIMENTAL RESULTS

In this section, the observed behavior and modes of failure for each wall will be described. Two types of composite fabrics were used in the present study; a 611 g/m² (18 oz/yd²) unidirectional glass fabric was bonded to the north and south faces of specimens S75/25 and S20/40. For specimen S30/30, a 611 g/m² (18 oz/yd²) cross-ply (i.e., 0/90) fabric was used.

A primer was applied to the wall surfaces, and the composite strips were saturated and bonded to the wall with a two-component epoxy resin.

A symmetrically retrofitted wall was tested, and a similar response was observed for the positive and negative directions of loading (Velazquez-Dimas et al. 1999). Consequently, in order to obtain the maximum amount of information from a limited number of specimens, two of the test specimens were retrofitted with different amounts of reinforcement on each face. Low reinforcement ratios were used because they were felt to be sufficient for strengthening URM walls with low height-to-thickness ratios against seismic loads.

The observed behavior of the tested walls will be explained as follows. First, the behavior of one of the walls (S75/25) will be discussed in detail. This will be followed by a brief description of the other two walls. Finally, the overall behavior of the three tested walls will be compared.

Wall S75/25

To determine the load-carrying capacity of plane brickwork, this wall was first tested as a control specimen (without any composite strips). Under these conditions, the wall failed at an applied pressure of 4.13 kPa (0.6 psi) by splitting in two pieces, as depicted in Fig. 5. The wall was later retrofitted and tested again. This specimen had reinforcement ratios of 25% and 75% of the balanced condition for the south and the north faces, respectively. The south face was subjected to 21 cycles of loading, while the north face supported 23 cycles. The behavior on both faces was characterized by progressive bed joint cracking and gradual delamination of the composite strips

(a)
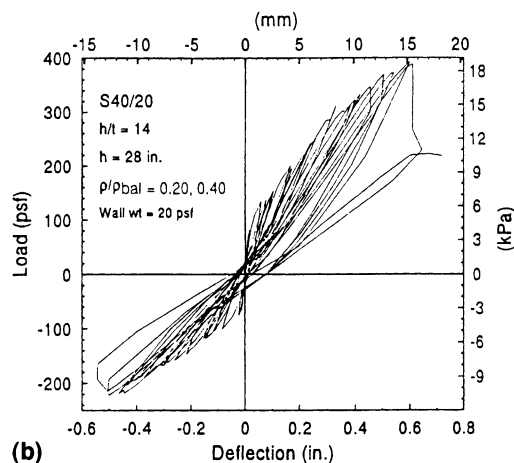
(b)

FIG. 7. Specimen S40/20: (a) Cracking and Delamination Pattern at Failure on South Face; (b) Load versus Deflection at Midheight

as the applied pressure increased. Wider cracks were observed on the south face of the wall, where a 2 mm crack width was measured. Cracks spread for almost 75% of the wall area on both faces. Essentially, linear elastic behavior was observed before major crack development on both faces. This resulted in a stiffness degradation, as shown in Fig. 6(a).

The first major crack, the one that developed along the full bed joint, was detected below the middle bed joint on the south face during the fourth cycle at an applied pressure of 6.9 kPa (1.0 psi) and a deflection of 3.5 mm (0.14 in.). For the north face, the first major horizontal crack was detected during the fifth cycle above and below the middle brick course at a pressure of 12.61 kPa (1.83 psi) and a deflection of 3.8 mm (0.15 in.). The delamination process began at many points on the three composite strips of the south face during the eighth cycle at an applied pressure of 11.57 kPa (1.67 psi) and a deflection of 5 mm (0.2 in.). On the north face, the first delaminated area was marked on the central and the west strips at midheight during the 11th cycle at an applied pressure of 18.67 kPa (2.7 psi) and a deflection of 7.6 mm (0.3 in.); i.e., at pressure and deflection levels 50% higher than those measured for the south face. These two events are very important, since the most significant stiffness degradation of the wall is attributed to them.

Longitudinal tensile strain of 1% in the composite strips was measured on the south face of the wall. A compressive strain of 0.25% was also recorded for the same face. Maximum strains of 1.2% in tension and 0.3% in compression were measured in the composite strips of the north face. In Fig. 6(b), a typical load versus strain curve is shown.

Another piece of data collected was the wall rotation at the top and bottom ends. Rotations as much as 3.24° and 3.06° were recorded at the top support for both reinforcement ratios, as depicted in Fig. 6(c). Although the north face had three times more reinforcement than did the south face, the last values are fairly close. This is attributed to the excessive delamination suffered by the composite strips on both faces. Thus, the stiffness of the wall degrades to similar values for both faces once excessive delamination begins to control the wall behavior.

Different modes of failure occurred on both faces. Twenty-one cycles were applied to the south face. Due to the severe damage caused by delamination on the three strips, the test was terminated. The top half of the west strip was almost completely delaminated. The same situation was observed for the bottom-half area of the central strip. The east strip was almost fully delaminated from the top to the bottom support. Delamination started at midheight, then spread above and below the middle brick course. No tensile failure on the composite strips was reached due to the fact that the load was stopped at a pressure of 12.4 kPa (1.8 psi) and a maximum deflection of 16 mm (0.63 in.). This was done in order to continue the test for the north face.

Very stiff behavior was observed for the north face. The failure occurred by a sudden peeling of the three strips at the top support. On this face, delaminated areas were located mostly above the middle brick course, as shown in Fig. 6(d). This failure took place at a maximum pressure of 31.03 kPa (4.5 psi) and for an ultimate deflection of 15.5 mm (0.61 in.). Peeling controlled the mode of failure for both faces, although a tensile failure of the fabric was expected due to the relatively

TABLE 4. Summary of Test Results

Category (1)	Parameter (2)	Specimen S75/25		Specimen S20/40		Specimen S30/30	
		North face (3)	South face (4)	North face (5)	South face (6)	North face (7)	South face (8)
First major crack	Cycle	5	4	4	7	9.0 (187)	7
First major crack	Pressure [kPa (psf)]	12.6 (263)	6.9 (144)	5.1 (107)	9.6 (202)		10.3 (216)
First major crack	Deflection [mm (in.)]	3.8 (0.15)	3.5 (0.14)	2.5 (0.1)	4.2 (0.16)	2.5 (0.1)	3.8 (0.15)
First major crack	Location	Above and below central brick course	Below middle brick course	At center above and below midheight	Top bed joint of central brick course	Top bed joint of central brick course	Top bed joint of central brick course
First delamination	Cycle	11	8	8	12	12	11
First delamination	Pressure [kPa (psf)]	18.7 (389)	11.6 (245)	7 (145)	16.2 (346)	13 (274)	12.8 (274)
First delamination	Deflection [mm (in.)]	7.6 (0.3)	5 (0.2)	6.6 (0.26)	9.7 (0.4)	6.6 (0.26)	6.3 (0.25)
First delamination	Location	Central and west strips at center	West strip above and central strips below	East and west strips above and below center	Central and west strips above center	West strip two bricks above center	West strip two bricks below midheight
Maximum strain	Compression (%)	0.3	0.25	0.2	0.3	0.1	0.1
Maximum strain	Tension (%)	1.2	1.0	1.2	1.0	0.7	1.0
Maximum strain	Strip	Central at midheight	West at center, central at top	Central at midheight	Central at top	Central at midheight	Central at midheight
Maximum rotation	Top (°)	3.24	3.1	3.03	3.03	2.0	2.0
Mode of failure	Cycle	23	21	16	18	16	17
Mode of failure	Pressure [kPa (psf)]	31 (648)	12.4 (259)	10.3 (216)	18.6 (389)	15.5 (331)	16.6 (346)
Mode of failure	Deflection [mm (in.)]	15.5 (0.6)	16 (0.63)	12.5 (0.5)	15.2 (0.6)	8.9 (0.35)	10 (0.4)
Mode of failure	Type	FD	PD	PD	FD	NO	T
Mode of failure	Location	All strips top half part	All strips[a]	East strip top half part	All strips[b]	No failure	All strips at midheight
Span drift δ_{max}/h (%)	—	2.5	2.25	1.8	2.1	1.4	1.25
Ratio p_{max}/Wt	—	33	13	11	20	17	16

Note: D = delamination, T = tensile, C = compression, Wt = weight of the wall/ft^2, P = part, and F = full.
[a]West strip top half and central and east strips bottom half part.
[b]Fully peeled off for all strips; east and west strips bottom half and central strip top half.

low reinforcement ratios used. However, these peeling failures did not occur until the specimen had resisted significant load and displacement. In addition, the ratio of maximum supported lateral pressure for the north and the south face ($P_{maxN}/P_{maxS} = 2.5$) was in agreement with that given by the corresponding reinforcement ratios; i.e., close enough to 3. However, the same pressure ratio was not observed for the first major crack and the first delaminated area on both faces of the specimen.

Wall S20/40

This specimen was reinforced with 20% balanced reinforcement ratio on the north face, while 40% was used for the south face. Experimental results indicated that both faces exhibited a similar crack and delamination pattern. However, cracks were narrower on the south side, which in turn was stiffer. Crack patterns were more noticeable on the top half of the wall on both faces.

The modes of failure were as follows: For the north face, during the 16th cycle, a large delaminated area occurred on the east strip from the center to the top steel channel. The central and the west strips delaminated almost 50% of their own areas. Most of these delaminated areas were located above the middle brick course. Failure occurred on the south face during the 18th cycle on the three strips, which experienced peeling from the steel channel. The west and the east strips peeled off at the bottom support, and the central one at the top. No tensile failure on the fabric was observed. However, a wide longitudinal mortar joint crack developed along the bottom bed joint of the central brick course, as shown in Fig. 7(a). Fig. 7(b) shows the load versus deflection curve, where the failure on both faces is denoted by a sudden loss of wall stiffness at the corresponding hysteretic loop. Details about the overall behavior of both faces of this wall are summarized in Table 4.

Wall S30/30

Because the failure of the previous two walls was due to excessive delamination, this wall was retrofitted in a more efficient way. As a result, a lighter fabric was used. The fabric was an 18 oz cross-ply; i.e., the fabric density was reduced by 50% in the tested direction. Thus, with a 30% reinforcement ratio, vertical strips of 81 mm (3.2 in.) width were symmetrically bonded to the wall surfaces. Therefore, the width of the strips was increased by a factor of two, compared with the fabric used on the previous walls. By increasing the contact area, the interface shear stress was reduced; this prevented the delamination observed in previous walls and caused a tensile failure of the fabric. According to the experimental results, this wall posed stiffer behavior with respect to the others. The important aspects of the behavior of this specimen are shown in Table 4.

Fairly symmetrical behavior was experienced for this wall. Due to the good interface behavior observed on both wall faces, few delaminated areas developed, as shown in Fig. 8(a). Those were marked away from the center brick course and were caused either by an uneven brick surface or by a wide flexural crack. Cracks penetrated through the bed joint as much as 75% of the wall thickness. Tensile failure occurred during the 17th cycle on the south face on the three composite strips at midheight. At failure, this wall spilt into two pieces due to the wide horizontal crack that developed along the central bed joint just below the middle brick course [Fig. 8(b)]. Failure points were at the center for the central and east strips where the big crack developed. However, the west strip showed the largest delaminated area and broke below the central brick course where an uneven brick was located. The symmetrical behavior of this specimen can be seen in the load versus deflection curve shown in Fig. 8(c).

## DISCUSSION AND COMPARISON OF EXPERIMENTAL RESULTS

The three URM walls tested had the same height-to-thickness ratio ($h/t = 14$), and were retrofitted using the same epoxy and primer. Two different glass fabric densities and five reinforcement ratios were investigated. The load-deflection envelopes for the three walls are presented in Fig. 9. For nonsymmetrically retrofitted walls, the ultimate deflection was practically the same. However, within the range of reinforcement ratios investigated in the present study, the ratio of the
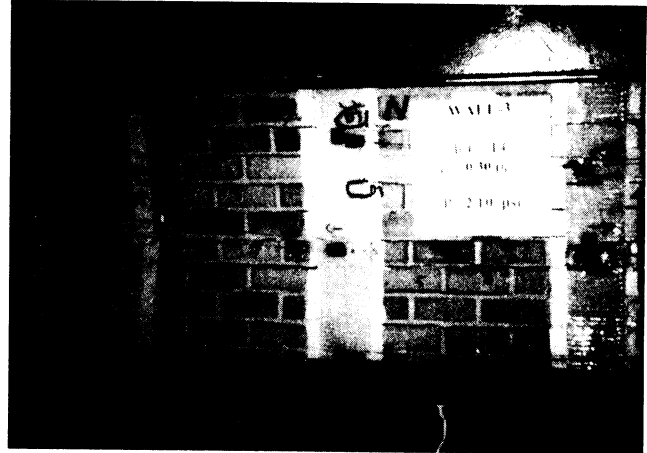
(a)
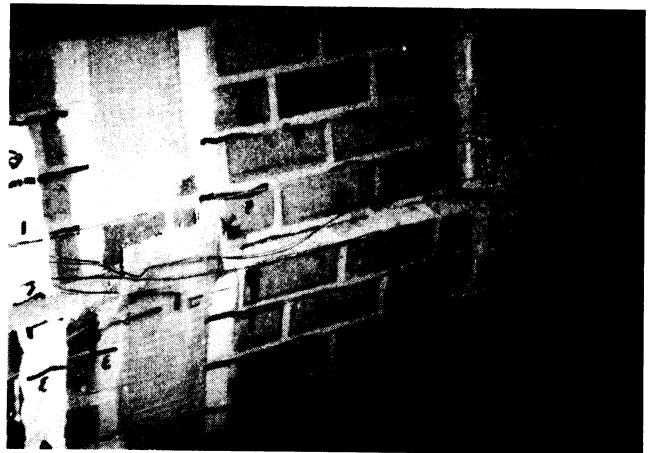
(b)
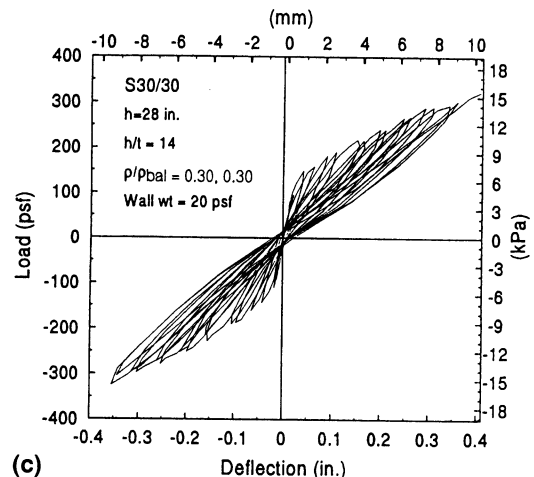
(c)

FIG. 8. Specimen S30/30: (a) Cracking and Delamination Pattern at Failure on North Face; (b) Tensile Failure of GFRP Strips on South Face; (c) Load versus Deflection at Midheight
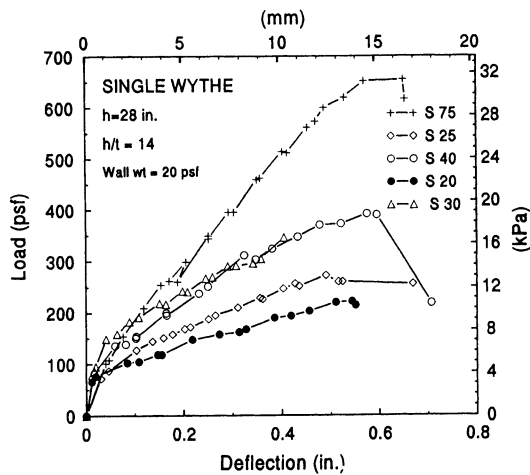
FIG. 9. Maximum Load Envelopes for All Test Specimens

maximum supported lateral pressure by each face of a given wall was proportional to the amount of reinforcement. For specimens retrofitted with unidirectional fabric, i.e., S75/25 and S20/40, the ultimate deflection appears to be independent of the reinforcement ratio. The longitudinal tensile strains on the composite fabrics were similar in all specimens; i.e., about 1%–1.2% for most cases.

The behavior of specimen S30/30, in which the shear transfer stresses were reduced by using wider fabric strips, was in many ways different from that of the other two walls. For example, the maximum rotation for this wall was about two-thirds that of the other walls. As can be seen in Fig. 9, walls S75/25 and S20/40 showed larger deflection capacity but less stiffness than wall S30/30. Walls S75/25 and S20/40 that were retrofitted with stronger fabric exhibited more delamination than wall S30/30, which was retrofitted with wider strips of fabric; the latter practically showed no delamination. Due to the ability to support larger deflections, the first two walls lasted through a larger number of loading cycles. Therefore, they dissipated more energy.

The water-based primer used on the tested walls gave good interface behavior, since all peeled composite strips took away the top brick surface. Failures due to excessive delamination proved to be a slowly progressing phenomenon, resulting in more dissipated energy when such failures took place. These delaminations generally took place at pressures much larger than those required by service conditions. Considering the hysteretic behavior of these specimens, failure of walls at higher load levels by delamination is more desirable than other modes of failure—for example, tension failure of GFRP strips at lower load levels.

CONCLUSIONS

From the observed behavior of this set of URM masonry walls retrofitted with GFRP vertical composite strips, the following conclusions can be drawn:

1. The ultimate flexural strength of the tested walls was significantly increased; the applied pressure varied from 10 to 32 times the unit weight of the wall per surface area.
2. Deflections as much as 2.5% of the wall height were observed for walls with unidirectional fabric; these walls deflected almost 14 times the maximum allowable deflection according to the latest masonry specifications.
3. Inelastic behavior was observed as a result of brickwork softening and delamination of the GFRP strips; this is of interest, considering that brick and composite strips, individually, behave in a brittle manner.

4. Weak shear transfer capacity of the brickwork controlled the mode of failure on walls retrofitted with unidirectional fabric.
5. Tensile failure of the GFRP strips was reached in specimen S30/30, where lighter fabric was used. However, the stiffer behavior of this specimen resulted in lower deflections.
6. GFRP composite strips proved to be a good alternative for retrofitting URM walls against lateral loads such as those from seismic forces.

ACKNOWLEDGMENTS

APPENDIX. REFERENCES

Abboud, B. E., Hamid, A. A., and Harris, H. G. (1990). "Small-scale modeling of concrete block masonry structures." *ACI Struct. J.*, 87(2).

Abrams, D. P., Angel, R., and Uzanski, J. (1993). "Transverse strength of damaged URM infills." *Proc., ASCE Struct. Congr.*, ASCE, Reston, Va.

Abrams, D. P., and Costley, A. C. (1996). "Seismic evaluation of unreinforced masonry buildings." *11th World Conf. on Earthquake Engrg.*, Paper No. 976.

Bennedetti, D., and Benzoni, G. M. (1984). "A numerical model for seismic analysis of masonry buildings: Experiments and correlations." *Earthquake Engrg. & Struct. Dyn.*, 12.

Bhende, D., and Ovadia, D. (1994). "Out-of-plane strengthening scheme for reinforced masonry walls." *Concrete Int.*, April, 30–34.

Bruneau, M. (1994). "Seismic evaluation of unreinforced masonry buildings: A state-of-the-art report." *Can J. Civ. Engrg.*, Ottawa, 21, 512–539.

Dawe, J. L., and Seah, C. K. (1989). "Out-of-plane of concrete masonry infilled panels." *Can J. Civ. Engrg.*, Ottawa, 16, 854–864.

Deppe, K. (1988). "The Whittier Narrows, California earthquake of October 1, 1987—Evaluation of strengthened unreinforced masonry in Los Angeles City." *Earthquake Spectra* 4(1), 157–179.

Drysdale, R. D., Hamid, A. A., and Bake, R. L. (1994). *Masonry structures behavior and design*. Prentice-Hall, Englewood Cliffs, N.J.

Ehsani, M. R., and Saadatmanesh, H. (1994). "Out-of-plane strength of unreinforced brickwork retrofitted with fiber composites." *Proc., NCEER Workshop on Seismic Response of Masonry Infills*, National Center for Earthquake Engineering Research, State University of New York at Buffalo.

Ehsani, M. R., and Saadatmanesh, H. (1996). "Seismic retrofitting of URM walls with fiber composites." *Masonry Soc. J.*, 14(2), 63–72.

Ehsani, M. R., and Saadatmanesh, H. (1997). "Fiber composites: An economical alternative for retrofitting earthquake-damaged precast-concrete walls." *Earthquake Spectra*, 13(2), 225–241.

Essaway, A. M. (1986). "Strength of hallow Concrete block masonry walls subjected to lateral (out-of-plane) loading," PhD thesis, McMaster University, Canada.

Expected seismic performance of buildings. (1994). Earthquake Engineering Research Institute Ad Hoc Committee on Seismic Performance, El Cerrito, Calif.

Flanagan, R. D., Bennett, R. M., and Beavers, J. E. (1993). "Seismic behavior of unreinforced hallow clay tile infilled frames." *Masonry design and construction problems and repair, ASTM STP 1180*, ASTM, West Conshohoken, Pa.

Hamid, A. A., Chia-Calabria, C., and Harris, G. H. (1992). "Flexural behavior of joint reinforced block masonry walls." *ACI Struct. J.*, 89(1), 20–26.

Handbook for seismic rehabilitation of existing buildings. (1992). *FEMA-127*, Federal Emergency Management Agency, Washington, D.C.

Hendry, A. W. (1973). "The lateral strength of unreinforced brickwork." *Struct. Engrg. J.*, 51, 42–50.

Kehoe, B. E. (1996). "Performance of retrofitted unreinforced masonry buildings." *11th World Conf. on Earthquake Engrg.*, Paper No. 1417.

Laursen, P. T., Seible, F., Hegemier, G. A., and Innamorato, D. (1995).

"Seismic retrofit and repair of masonry walls with carbon overlays." *Non-metallic (FRP) reinforcement for concrete structures*. Reunion Internationale des Laboratoires d'Essais et de Recherches sur les Materiaux et les Constructions.

Lester, J. (1998). "Staking your claim." *Civ. Engrg.*, ASCE, July, 65–67.

Lizundia, B., Holmes, W. T., Longstreth, M., and Kren, A. (1997). "Development of procedures to enhance the performance of rehabilitated URM buildings." *NIST GCR 97-724-1*, National Institute of Standards and Technology, Building and Fire Research Laboratory, Gaithersburg, Md.

"Methodology for mitigation of seismic hazard in existing unreinforced masonry buildings: Wall testing out-of-plane." (1981). *ABK-TR-04*. El Segundo, Calif.

Schwegler, G. (1995). "Masonry construction strengthened with fiber composites in seismically endangered zones." *10th Eur. Conf. on Earthquake Engrg.*, 2299–2303.

Schwegler, G., and Kelterborn, P. (1996). "Earthquake resistance of masonry structures strengthened with fiber composites." *11th World Conf. on Earthquake Engrg., Paper No. 1460.*

Siegel, H. I., and Fowler, L. W. (1994). "Jackson Brewery: Upgrading historic unreinforced brick buildings." *Earthquake Spectra*, 10(1).

Sucuoglu, H., and McNiven, H. D. (1991). "Seismic shear capacity of reinforced masonry piers." *J. Struct. Engrg.*, ASCE 117(7), 2166–2186.

Tobriner, S. M. (1984). "At earthquakes: 1755–1907." *Earthquake Spectra*, 1(1), 125–149.

Tomazevic, M. (1996). "Recent advances in earthquake-resistant design of masonry buildings: European prospective." *11th World Conf. on Earthquake Engrg., Paper No. 2012.*

Uniform code for building conservation. (1994). International Conference of Building Officials, Whittier, Calif.

Velazquez-Dimas, J. I. (1998). "Out-of-plane cyclic behavior of URM walls retrofitted with fiber composites," PhD dissertation, Department of Civil Engineering and Engineering Mechanics, University of Arizona, Tucson.

Velazquez-Dimas, J. I., Ehsani, M. R., and Saadatmanesh, H. (1999). "Out-of-plane behavior of brick masonry walls strengthened with fiber composites." *Earthquake Spectra*, in press.

Weeks, J., Seible, F., Hegemier, G., and Pristley, M. J. N. (1994). "The U.S.-TCCMAR full-scale five-story masonry research building test." University of California, San Diego.